Journal of Molecular Structure 1286 (2023) 135574

Contents lists available at ScienceDirect

Journal of Molecular Structure

journal homepage: www.elsevier.com/locate/molstr

Thoughtful investigation of ZnO doped Mg and co-doped Mg/Mn, Mg/Mn/F thin films: A first study

Warda Darenfad [a,*], Noubeil Guermat [b], Kamel Mirouh [a]

[a] Thin Films and Interfaces Laboratory (LCMI), University of Constantine 1, Constantine 25000, Algeria
[b] Department of Electronics, Faculty of Technology, University of M'sila, M'sila 28000, Algeria

ARTICLE INFO

Keywords:
ZnO
Mg-doped ZnO
Mg/Mn co-doped ZnO
Mg/Mn/F co-doped ZnO
Spray pyrolysis
SEM
Electrical and optical properties

ABSTRACT

Pure ZnO, $Zn_{0.97}Mg_{0.03}O$, $Zn_{0.96}Mg_{0.03}Mn_{0.01}O$ and $Zn_{0.90}Mg_{0.03}Mn_{0.01}F_{0.06}O$ nanocrystalline thin films were successfully elaborated on glass substrates using spray pyrolysis method. Structural proprieties were mainly investigated by X-ray diffractometer (XRD), Scanning electron microscopy (SEM), UV–Visible spectrophotometry and Hall effect measurement technique. The XRD spectra revealed the preferred orientation of the prepared polycrystalline along (002) reflection and showed the hexagonal wurtzite structure. A decrease in the crystallinity of $Zn_{0.90}Mg_{0.03}Mn_{0.01}F_{0.06}O$ sample has been observed from 17.206 to 13.489 nm due to the change in its ionic size. SEM images highlighted the homogeneity of the prepared samples surface and proved their nanostructure morphology. For the doped 3%Mg, 1%Mn and 6%F polycrystalline, the obtained transmission spectra were higher than that of pure ZnO and a shift towards the lower wavelengths with a band gap of 3.31 eV has been observed for $Zn_{0.97}Mg_{0.03}O$ film. A low electrical resistivity of about 1.33×10^{-3} Ω.cm was measured for $Zn_{0.90}Mg_{0.03}Mn_{0.01}F_{0.06}O$ thin film. Also, its photoelectric performance was proven to be significantly higher than that of the previously reported ZnO doped and co-doped thin films, which makes it a remarkable candidate for several optoelectronic devices.

1. Introduction

Transparent oxides with high electrical conductivity are generating considerable interest because of their potential for various applications such as: microelectronics, mechanics, optoelectronics, surface treatment, etc. A good transparent conductive oxide (TCO) is defined by its high electrical conductivity and low absorption rate in visible light; also its high reflection in the infrared. The most well-known transparent conductive oxides are: Zinc, Cadmium, Tin, Indium and Gallium oxides. Among these TCOs, the present paper aims to shed new light on the zinc oxide (ZnO). Many attempts have been made to enhance its optical and electrical proprieties; like doping and co-doping ZnO thin films with suitable transition metals, rare and noble metals, to ensure ZnO as a promising material for optoelectronic applications [1]. These properties could be further improved by varying the stoichiometric ratio of the doping element in the host material [2].Therefore, the selection of this doping is important to obtain a wider range of possible applications. As many researchers have highlighted, the luminescence properties of ZnO thin films could be improved by doping it with indium (In) and gallium (Ga). However, these dopants have some major flaws regarding their high prices and toxicity compared to other dopants. In this paper, we use as alternative dopants, the Magnesium (Mg), Manganese (Mn) and Fluorine (F). Firstly, doping with Mg has been decided for many reasons: (i) a solid solution of MgO (Eg = 7.8 eV) and ZnO helps to increase the band gap and UV-vis luminescence intensity of ZnO: Mg films [3]; (ii) the incorporation of Mg into Zn leaves the lattice constants almost invariant; (iii) the ionic radius of Mg^{+2} (0.066 nm) is very close to Zn^{+2} (0.074 nm) which allows Mg to substitute Zn in the lattice; (iv) abundant [4]; (v) non-toxic and cheap [4]. In a previous work, we reported that ZnO doped with 1% Mg exhibits good transmittance (85%) with an increase in the optical gap [3]. However, the mixture of Mg and ZnO does not increase the additional carriers; it improves the scattering centre and reduces the carrier's mobility [5]. Furthermore, the addition of other impurity atoms in $Zn_{1-x}Mg_xO$ increases its conductivity [5]. Secondly, Manganese has been chosen as a dopant because: (i) the similarity in ionic radius of Mn and Zn atoms results in a higher solubility of Mn in the ZnO crystal lattice [6]; (ii) the ZnO semiconductor with a band gap of 3.3 eV is suitable for different applications but the addition of Mn helps to improve its proprieties by tuning its size and band gap [7]; (iii) the convenience of d-electrons at the t2g level that can join the ZnO valance

* Corresponding author.
E-mail address: daranfed.warda@umc.edu.dz (W. Darenfad).

https://doi.org/10.1016/j.molstruc.2023.135574
Received 27 November 2022; Received in revised form 2 April 2023; Accepted 13 April 2023
Available online 22 April 2023

bond [7]. In addition, Mn concentration is limited to 1% in this work to avoid generating secondary phase training. Subbiah et al. [8] pointed out that the addition of Mg in the $Zn_{1-X}Mn_XO$ mix adjusts the optical properties. Thirdly, the ionic radii of F^{-1} (0.131 nm) is close to O^{-2} (0.138 nm). Thus, the substitution of oxygen atoms by F in the ZnO lattice could improve the electron mobility as well as the transparency according to the following relation [9]:

$$O^x + F^- \rightarrow F\cdot + e^- \quad (1)$$

For these reasons, several works in recent years have focused on the effect of co-doping using fluorine and other dopants [10,11]. For example, Pan et al. [10] prepared pure ZnO and fluorine (F) /tin (Sn) co-doped ZnO (FTZO) on glass substrates by the sol–gel processing. Performance comparisons found that a minimum resistivity of about 1×10^{-3} Ω.cm, obtained for the FTZO thin film with 3% F doping, and the average optical transmittance in the entire visible wavelength region was higher than 90%. Mallick et al. [12] deposited thin films of Sn-doped and Sn-F co-doped ZnO by the pulsed laser deposition (PLD) technique, where fluorine co-doping leads to a decrease in resistivity compared to Zn-doped ZnO. However, Starowicz et al. [11] reported on the deposition of ZnO films doped and co-doped with Al and Al-F, respectively. They reported an increase in the resistivity value of the co-doped film. However, the effects of fluorine co-doping versus doped films on physical characteristics is not yet clear. The spray pyrolysis method is used in this work due to the possibility of using precursors of high purity, ease of deposition on large surfaces substrates and complex shape at various temperatures and to their low cost. To our knowledge, there are no reported works on zinc oxide co-doped with Magnesium, Manganese and Fluorine (ZnO/Mg/Mn/F) thin films elaborated by physical or chemical methods for the fabrication of TCO films for solar cells application.

The present work aims to improve the electrical conductivity and to ensure a high light transmission of thin films of ZnO co-doped Mg/Mn/F. Also, this study is carried out for further improvement of the material physical properties in order to be used as a conductive transparent layer in thin film solar cells.

2. Experimental details

The thin layers of undoped, Mg-doped, co-doped (Mg-Mn) and co-doped (Mg, Mn and F) ZnO were deposited by the reactive chemical spraying technique (Spray pyrolysis) on a glass substrate. Before deposition process, the substrates were cleaned with acetone, rinsed in distilled water, then cleaned with ethanol and finally with distilled water. The spray solution was prepared from a mixture of zinc acetate dihydrate ($(Zn(CH_3COO)_2.2H_2O)$ mass 2.106 g and methanol (CH_3OH). Magnesium acetate tetrahydrate ($Mg(CH_3COO)_2.4H_2O$) was used as a dopant with a concentration of 3% to prepare the Mg-doped ZnO ($Zn_{0.97}Mg_{0.03}O$) thin films as well as manganese (II) acetate tetrahydrate ($Mn(CH_3COO)_2.4H_2O$) was used as a dopant with a concentration of 1% to prepare the thin layer of Mg-Mn co-doped ZnO ($Zn_{0.96}Mg_{0.03}Mn_{0.01}O$). Thin films of Mg-Mn and F co-doped ZnO ($Zn_{0.90}Mg_{0.03}Mn_{0.01}F_{0.06}$ O) were prepared by dissolving zinc acetate, 3% magnesium acetate tetrahydrate, 1% manganese (II) acetate tetrahydrate and 6% ammonium fluoride (NH_4F) in methanol.

All layers were elaborated under the same conditions shown in Table 1.

Table 1
Optimized deposit conditions.

Process parameters	Deposit conditions
Deposition temperature	400 °C
Solution flow	8 ml/min
Air flow	1 bar
Substrate-nozzle distance	17 cm

The crystalline structure of the prepared thin films was analyzed by a Philips X'Pert-PRO model PW3040 diffractometer with a Cu Kα radiation source (λ = 1.542 Å). Their morphology was investigated by FEI Quanta 450 FEG scanning electron microscope. The optical properties were studied using Shimadzu, model UV-3101PC UV–Vis-NIR spectrophotometer in the wavelength range of 300–800 nm. The Ecopia HMS-3000 system equipped with a magnet which produces a 1 T field during sample electrical measurements using a dedicated support. The device, consisting of four points arranged in a square geometry and connected to a generator is a complete system for measuring resistivity (ρ), the Hall coefficient, the concentration of carriers (n) and their mobility (μ).

3. Results and discussion

The XRD patterns observed for pure, Mg-doped, Mg/Mn co-doped and Mg/Mn/F co-doped ZnO polycrystalline are presented in Fig. 1. XRD spectra showed the same diffraction peaks for all the prepared thin films at 32.01°, 34.16°, 35.89°, 47.30°, 56.40°, 62.40° and 67.38°, which are attributed to (100), (002), (101), (102), (110), (103) and (200) reflections, respectively. They are indexed to hexagonal Wurtzite (WZ) structure according to the standard JCPDS card n° 36–1451 [13]. Moreover, it can be seen that no obvious peak related to Mg/Mn/F dopants or their oxides as well as no characteristic peaks for impurity are found which proves the purity of our elaborated polycrystalline. Also the existing hexagonal structure was not altered due to Mn/Mg or Mg/Mn/F doping. To evaluate the influence of the addition of Mg/Mn/F to ZnO on the intensity and the position of the (002) peak, a zoom of this peak for 2θ between 33.5° and 36° is carried out, as illustrated in Fig. 2. The initial doping of Mg increases the intensity of the (002) peak to its maximum, while the co-dopings of Mg/Mn and Mg/Mn/F lead to a decrease in intensity, indicating the reasonable loss of crystallinity due to the distortion of the lattice $Zn_{0.96}Mg_{0.03}Mn_{0.01}O$ and $Zn_{0.90}Mg_{0.03}Mn_{0.01}F_{0.06}O$ by the substitution of Mn and F. Moreover, we notice in Fig. 2 that the peak position is shifted to the lower 2θ side for Mg/Mn/F co-doping compared to mono-doping and Mg/Mn co-doping, which can be attributed to the replacement of Zn^{+2} ions by Mg^{+2}/Mn^{+2}/F^- ions.

The crystallite size (D) of our samples was estimated using the Scherer equation for the most intense peak [1]. The estimated crystallite sizes were grouped in Table 2. The results reveal that the initial doping of 3% Mg has increased D from 17.206 nm to 17.240 nm. Similar behavior has been reported by other authors on Mg-doped ZnO film enhancement [14–16]. Due to the divergence of ionic radius of 'Mg' and 'Zn' residual strain that is produced in the parent ZnO system [15]. The increase of crystallite size indicated that Mg doping may enhance the grain growth. Also, the segregation of Mg dopants in the grain boundaries and a large number of dislocations originated from dopant atoms in the interstitial sites also affect the crystal growth [14]. Moreover, after co-doping ZnO:3%Mg with 1%Mn or 1%Mn/6%F, the crystallite size decreased from 17.240 to 17.063 then 13.489 nm, respectively. This decrease can be attributed to the nucleation generated by the presence of Manganese (Mn) and Fluorine (F) at this doping order. Wang et al. has reported similar decrease in the crystallite size with Mg/F co-doped ZnO [17]. According to Wang et al. [17], the fluorine atoms occupy interstitial sites instead of substituting oxygen atoms, which results in a large number of dislocations that we may have as well in our case (Table 2).

SEM images of the pure ZnO, $Zn_{0.97}Mg_{0.03}O$, $Zn_{0.96}Mg_{0.03}Mn_{0.01}O$ and $Zn_{0.90}Mg_{0.03}Mn_{0.01}F_{0.06}O$ thin films are presented in Fig. 3. SEM images revealed that the prepared films display a homogeneous surface with nanostructured morphology. Fig. 3(a) showed that pure ZnO thin film is composed of numerous islands of irregular shapes. After doping with Mg (Fig. 3(b)), its morphology has changed to irregular grains. Likewise, for ZnO co-doped with Mg/Mn, (Fig. 3(c)) illustrated that the surface became more homogeneous, compact and dense with a nanometric granular structure. Nevertheless, the co-doping of ZnO with Mg/Mn/F (Fig. 3(d)) indicated that islands of irregular shapes were

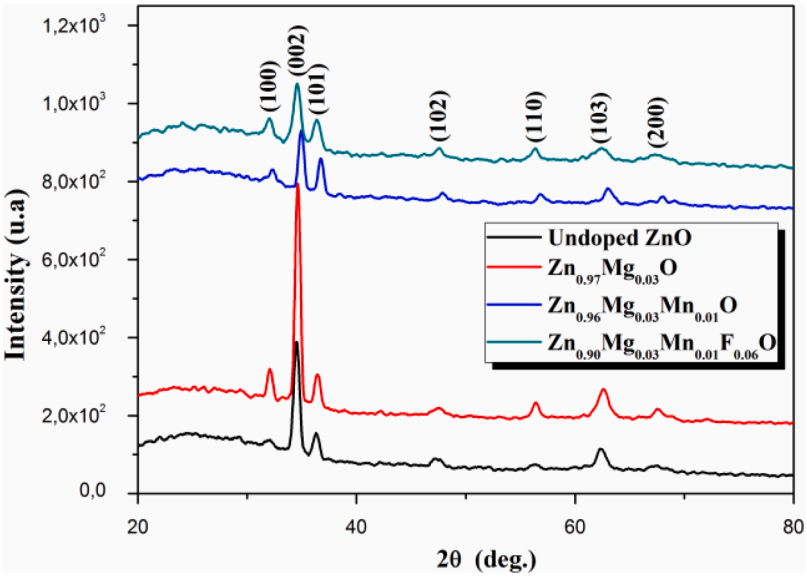

Fig. 1. XRD patterns of pure ZnO, $Zn_{0.97}Mg_{0.03}O$, $Zn_{0.96}Mg_{0.03}Mn_{0.01}O$ and $Zn_{0.90}Mg_{0.03}Mn_{0.01}F_{0.06}O$ thin films.

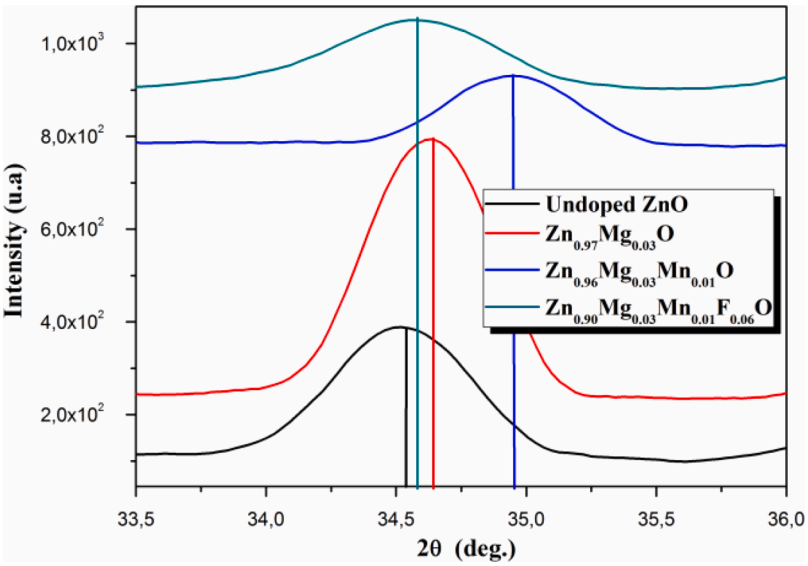

Fig. 2. The variation of XRD peak position and intensity along (002) plane from 33.5° to 36° of our films.

Table 2
The variation in crystallite size, FWHM, dislocation density and strain of pure, doped and co-doped ZnO thin films.

Sample	Crystallite size, D (nm)	FWHM, β (°)	Dislocation density, δ $(nm)^{-2}$	Strain, ε (10^{-3})
ZnO	17.206	0.48406	0.00337	2.0144
$Zn_{0.97}Mg_{0.03}O$	17.240	0.48288	0.00336	2.0104
$Zn_{0.96}Mg_{0.03}Mn_{0.01}O$	17.063	0.48830	0.00343	2.0312
$Zn_{0.90}Mg_{0.03}Mn_{0.01}F_{0.06}O$	13.489	0.61707	0.00549	2.5695

transformed to nearly lamellar/elliptic nanostructure with an average size of 50 nm. According to the literature, this shape is efficient to trap light which could be useful for solar cells [18].

We investigated the composition and elements state of our films (Fig. 4(e)-(d)). EDAX data exposed the presence of Zn and O elements in the pure ZnO thin film. Unmistakably, a clear Mg peaks has appeared along with the Zn and O (Fig. 4(b)) in $Zn_{0.97}Mg_{0.03}O$. As in Fig. 4(c), the addition of Mg and Mn to ZnO is considered successful with the presence of Mg (8.369 at.%) and Mn (2.457 at%). Lastly for the ZnO co-doping with Mg/Mn/F (Fig. 4(d)), the appearance of Mg, Mn and F peaks confirmed the good dispersion of these precursors into ZnO lattice. EDAX results are in a good agreement with XRD data which proves that Mg, Mn and F are not separated from ZnO matrix.

The optical transmission spectra at room temperature of the films are shown in Fig. 5. According to Fig. 5, the fabricated samples have a high transparency in the visible region with an average transmission of 85.99% (Table 3), which demonstrates the unvarying structure and smooth surface of the films [19]. This further confirms the previous results. Moreover, the transmission is slightly amplified by the addition of metal precursors compared to that of pure ZnO, because of the good integration of Mg, Mn and F into ZnO matrix. The high transmittance (91.06%) of Mg-doped sample could be justified by the replacement of Zn by Mg in the crystal lattice, since MgO could broaden the optical band gap of the films and reduce the energy consumed by the photon transition [19]. Beside, the 3%Mg doped ZnO has a better crystallinity and

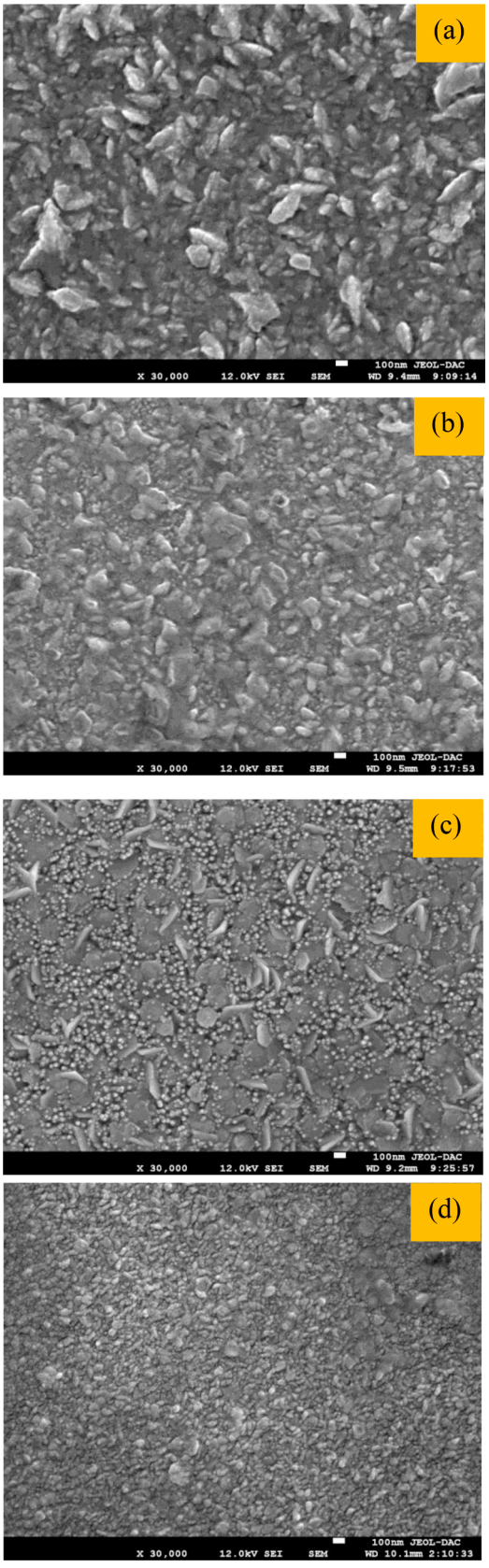

Fig. 3. SEM of (a) pure ZnO, (b) $Zn_{0.97}Mg_{0.03}O$, (c) $Zn_{0.96}Mg_{0.03}Mn_{0.01}O$ and (d) $Zn_{0.90}Mg_{0.03}Mn_{0.01}F_{0.06}$ O prepared thin films.

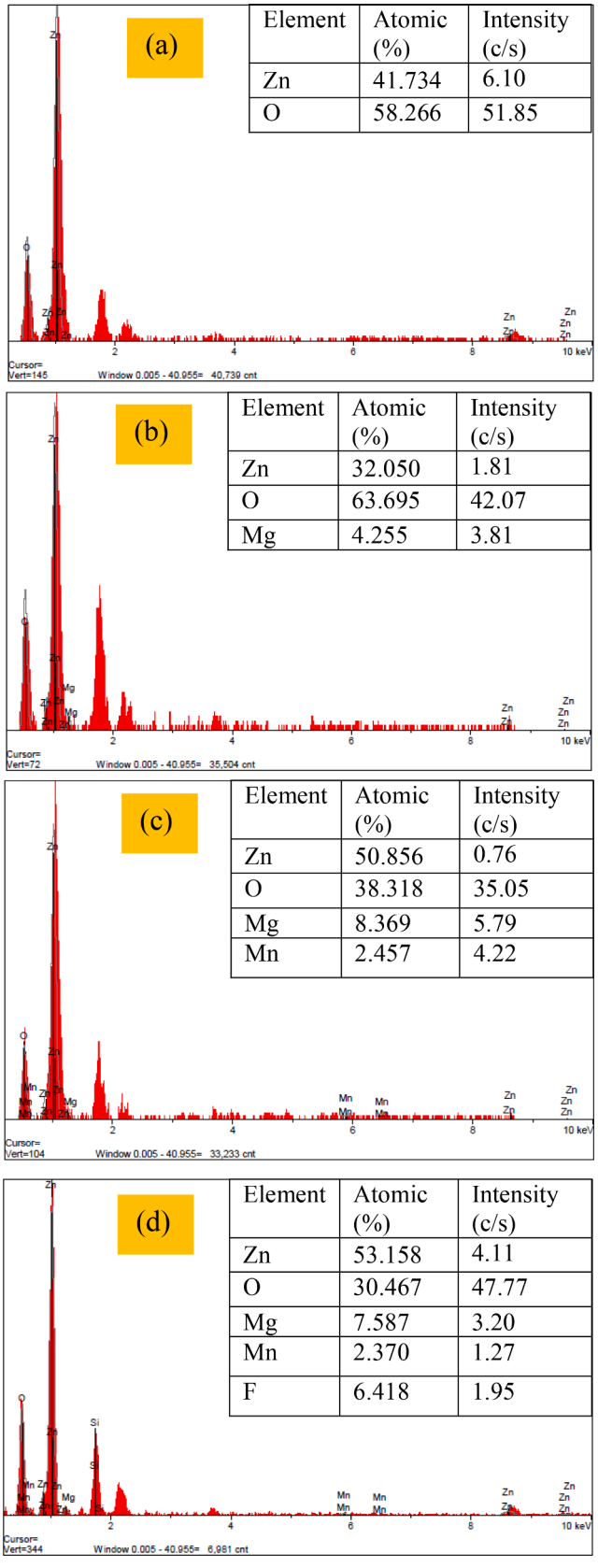

Fig. 4. EDAX spectrum of (a) pure ZnO, (b) $Zn_{0.97}Mg_{0.03}O$, (c) $Zn_{0.96}Mg_{0.03}Mn_{0.01}O$ and (d) $Zn_{0.90}Mg_{0.03}Mn_{0.01}F_{0.06}$ O thin films.

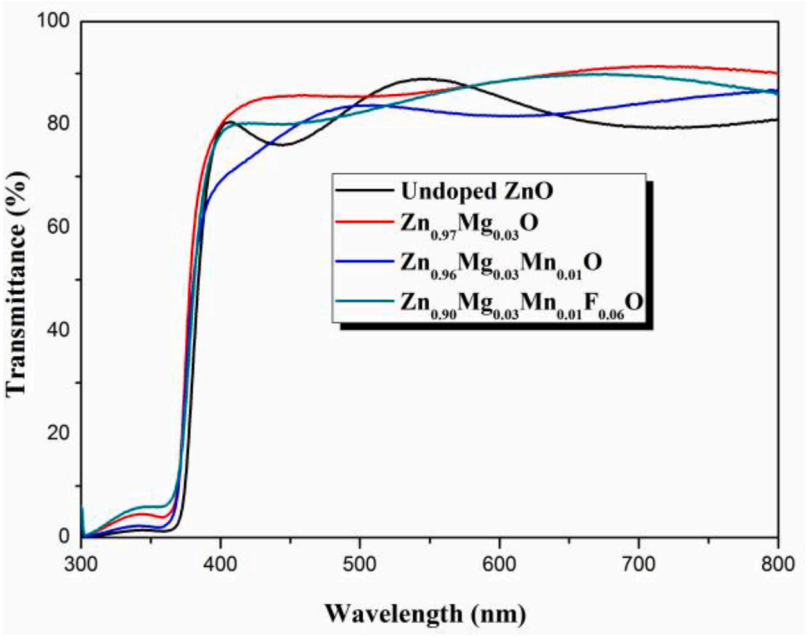

Fig. 5. Transmittance spectra of ZnO thin films with different doping ratios of Mg, Mn and F.

Table 3
Transmission values in the visible region of our films.

Sample	Max. Transmittance for Wavelength = 700 nm, (%)	Thickness, (nm)
ZnO	79.39	439
$Zn_{0.97}Mg_{0.03}O$	91.06	301
$Zn_{0.96}Mg_{0.03}Mn_{0.01}O$	84.01	487
$Zn_{0.90}Mg_{0.03}Mn_{0.01}F_{0.06}O$	89.53	454

doping efficiency compared to the other samples (Table 2). High transmittance is an advantageous feature for thin-film solar cell applications since it allows more high-energy photons to hit the solar cell. Hence, the slight decrease in the transmittance can be ascribed to the co-doping that lowers the crystallinity which correlates well with the earlier XRD results. Furthermore, this decrease can be explained by the increase in grain boundaries. The latter increases the scattering of light which will lead to a decrease in transmission [20].

To calculate the optical band gap energy for all our samples, the Tauc plot equation was used [21–23]. The plot $(\alpha h\upsilon)^2$ as a function of photon energy $(h\upsilon)$ is presented in Fig. 6.

$$(\alpha hv)^n = B\left(hv - E_g\right) \quad (2)$$

Where: E_g is the optical gap energy, α is the absorption coefficient, B is constant and $h\upsilon$ is the energy of the incident photon.

The band gap was found to be 3.22, 3.31, 3.24, and 3.27 eV for pure, Mg-doped, Mg/Mn co-doped and Mg/Mn/F co-doped ZnO thin films, respectively. Evidently, the optical band gap increases with the addition of Mg or Mg/Mn or Mg/Mn/F in the ZnO film. This increase is attributed to the Burstein-Moss effect, where, the introduction of new elements in the ZnO lattice creates new defects as a result of the difference in their electronegativity and ion radii. Furthermore, the success full

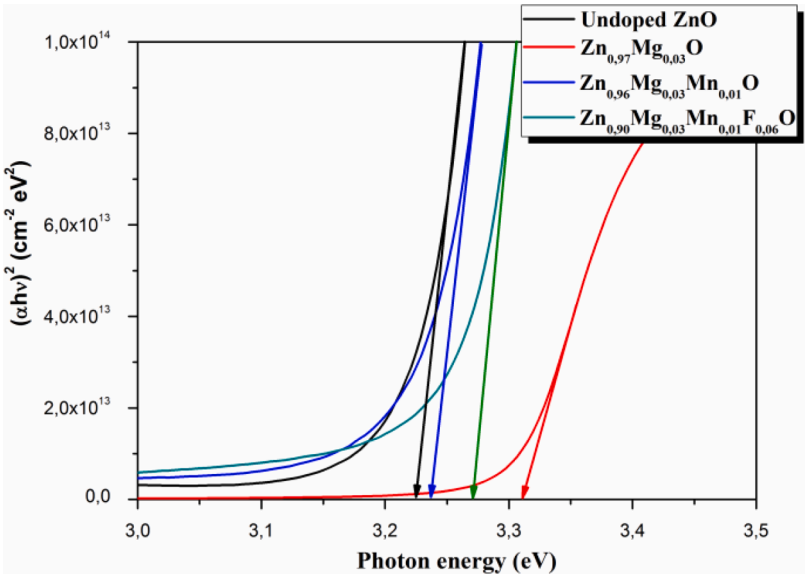

Fig. 6. The $(\alpha h\upsilon)^2$ versus hυ curves of ZnO thin films deposited with different dopant for the optical energy gap calculation.

incorporation of Mg and/or Mn and/or F into ZnO, creates more oxygen vacancies in ZnO lattice. These oxygen vacancies act as donors in the system and become positively charged releasing electrons into the conduction band. When the concentration of electron carriers exceeds the density of states of the edges of the conduction band, the Fermi level is pushed to move into the conduction band [2]. This Burstein-Moss shift leads to the observed widening of the band gap of our films. These results are in a good accordance with those published by several authors [24–27]. Yet, the same table showed a diminution in the optical gap for the co-doping $Zn_{0.96}Mg_{0.03}Mn_{0.01}O$ compared to $Zn_{0.97}Mg_{0.03}O$. The optical gap is decreased due to the band narrowing effect as the carrier concentration increases. This can be explained by the existence of electronic defects in the forbidden band. Transitions at photon energies lower than that of the gap will then be detected [28]. This decrease of the band gap energy for ZnO co-doped Mg/Mn was detected by Subbiah et al. [29]. They accredited this reduction to the development of new electronic states in the band gap [29].

Another significant parameter to characterize the disorder of a material is the Urbach tail energy (E_U). According to Urbach's law, the expression of the absorption coefficient (α) is as follows [30,31]:

$$\alpha = \alpha_0 \exp\left(\frac{h\nu}{E_u}\right) \quad (3)$$

Where: α_0 is a constant.

By plotting ln(α) as a function of hν (Fig. 7), one can assess the Urbach energy values for our synthesized films. The Urbach energy values of ZnO, $Zn_{0.970}Mg_{0.03}O$, $Zn_{0.96}Mg_{0.03}Mn_{0.01}O$ and $Zn_{0.90}Mg_{0.03}Mn_{0.01}F_{0.06}O$ thin films are listed in Table 4.

The Urbach energy varies with the concentration of doping and co-doping and shows a minimum value of 313.577 meV for concentration of 3% Mg. Though, this reduction in the Urbach energy demonstrated the improvement in the quality of the $Zn_{0.97}Mg_{0.03}O$ layer. On the other hand, for $Zn_{0.90}Mg_{0.03}Mn_{0.01}F_{0.06}O$ film we have the highest value of about 332.568 meV. This performance is undoubtedly due to the addition of F with the Mg and Mn atoms that does not take the necessary time to reorganize and occupy stable and favorable sites, which leads to the appearance of a large density of structural defects characterized by strong Urbach energy in the film lattice.

The electrical resistivity as a function of the doping and co-doping proportions is presented in Fig. 8. It could be noticed that the electrical resistivity of the film depends on the amount of Mg and/or Mn and/or F. Hence, with the addition of Mg to ZnO, an increase in the thin layer resistivity has been observed. Nonetheless, the resistivity of the

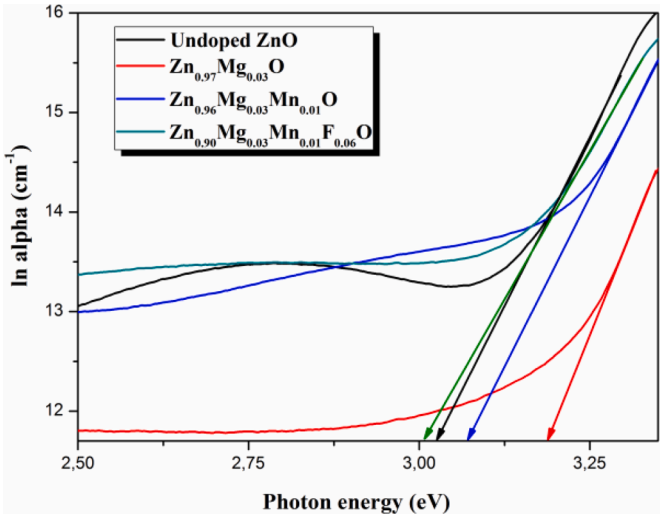

Fig. 7. Plots of ln(α) versus photon energy to determine the Urbach energy of ZnO thin films deposited with different dopant.

Table 4
Values of band gap energy and urbach energy of ZnO thin films deposited with different dopant obtained from Tauc plot expression.

Sample	Optical gap, (eV)	Urbach energy, (meV)
ZnO	3.22	330.360
$Zn_{0.97}Mg_{0.03}O$	3.31	313.577
$Zn_{0.96}Mg_{0.03}Mn_{0.01}O$	3.24	325.732
$Zn_{0.90}Mg_{0.03}Mn_{0.01}F_{0.06}$ O	3.27	332.568

samples diminished further with the co-dopants Mg/Mn and Mg/Mn/F and reaches its lowest value of 1.33×10^{-3} Ω.cm while the carrier concentration augmented to 3.1×10^{21} cm^{-3} for the $Zn_{0.90}Mg_{0.03}Mn_{0.01}F_{0.06}O$ film. This decrease in resistivity with the co-dopants is explained by the increase in the number of charge carriers (electrons) coming from the cations (Mg^{+2}, Mn^{+2}) and the ion (F^{-}) as donors which are integrated in substitutional or cation interstitial sites of Zn^{+2}. As mentioned above, doping and co-doping causes disorder formation in the film network (Fig. 8). This disorder yields the appearance of defects by the introduction of ions dopants as a substitute for zinc or oxygen. The presence of these extrinsic defects lead to an n-type conduction, with an increase in the concentration of free carriers and consequently the conductivity.

Contrariwise, the ZnO resistivity increase with Mg doping is caused by the reduction of the disorder in the film (see Table 4). Consequently, the reorganization of the lattice is accompanied by a reduction of Zn atoms in the interstitial site, which causes a decrease in the free carriers, thus increases the resistivity. What is more, the introduction of Mg^{+2} to ZnO film lessens its tendency to form metal atom interstitial defects and oxygen vacancies and increases the energy formation. Instead, Mg^{+2} doping increases the band gap of the resulting solid because MgO has a wider band gap (7.8 eV) than that of ZnO (3.37 eV). Therefore, the diminution in defects and the increase in the bandgap both contribute to the increase in the resistivity of Mg-doped ZnO films. Darenfad et al. [3], Huang et al. [32] Kaushal et al. [33] and Babur et al. [34] reported a similar resistivity evolution. A comparison of optical and electrical properties of the $Zn_{0.90}Mg_{0.03}Mn_{0.01}F_{0.06}O$ film with previous reports elaborated with different methods is summarized in Table 5. This table featured the improvement of electrical properties with the addition of fluorine as a dopant to ZnO:Mg:Mn lattice as a result of the charge concentration amplification compared to other films deposited by different methods.

4. Conclusion

Pure ZnO, $Zn_{0.970}Mg_{0.03}O$, $Zn_{0.96}Mg_{0.03}Mn_{0.01}O$ and $Zn_{0.90}Mg_{0.03}Mn_{0.01}F_{0.06}O$ thin films were deposited by the spray pyrolysis technique. The structural, morphological, optical, and electrical properties of the elaborated films were fully investigated. The XRD results revealed that the prepared polycrystalline films have a hexagonal wurtzite structure with (002) as the preferred orientation. The crystallite size of the ZnO film could be improved with the incorporation of Mg precursor compared to the other dopants. XRD and EDAX data confirmed the good dispersion of Mg, Mn and F atoms within ZnO lattice. The average optical transmittance in the entire visible wavelength region is higher than 85%. The band gap of ZnO is amplified by doping and co-doping, compared to the reference pure ZnO film. $Zn_{0.90}Mg_{0.03}Mn_{0.01}F_{0.06}O$ thin film has a low resistivity about 1.33×10^{-3} Ω.cm, with a carrier concentration of 3.1×10^{21} cm^{-3} and a Hall mobility of 6.33 cm^2 V^{-1} s^{-1}. These features may make $Zn_{0.90}Mg_{0.03}Mn_{0.01}F_{0.06}O$ an excellent transparent conducting electrode for optoelectronic devices.

Declaration of Competing Interest

The authors declare that they have no known competing financial

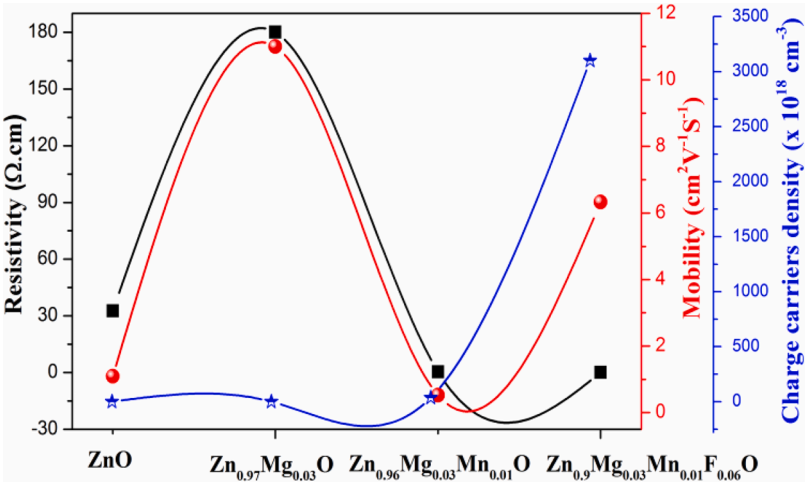

Fig. 8. Variation of resistivity (ρ), Hall mobility (μ) and carrier concentration (n) of ZnO films for different doping rates of Mg, Mn and F.

Table 5
A comparison of transmittance and electrical properties of (Mg/Mn/F) co-doped ZnO thin film with previous reports.

TCO Material	Technique of fabrication	T, (%)	Resistivity, (Ω.cm)	Ref.
$Zn_{0.99}Mg_{0.01}O$	Spray pyrolysis	84	–	[3]
$Zn_{0.96}Mg_{0.04}O$	Sol gel	85	2.5×10^{6}	[32]
ZnO:2 at% Mn	RF magnetron sputtering	85	3×10^{-1}	[35]
$Zn_{0.95}Ga_{0.03}F_{0.02}O$	RF magnetron sputtering	91.2	6.667×10^{-3}	[36]
$Zn_{0.91}Mg_{0.03}F_{0.06}O$	Spray pyrolysis	80	$1.11 \times 10^{+2}$	[3]
$Zn_{0.96}Ga_{0.02}Mg_{0.02}O$	RF magnetron sputterin	87.71	1.53×10^{-3}	[37]
ZnO:3 at.% In: 5 at.% F	Spray pyrolysis	82.1	5.2×10^{-2}	[38]
ZnO: 5 at% Mg:2 at%Ga	RF magnetron sputterin	85	5.76×10^{-3}	[39]
$Zn_{0.87}Fe_{0.05}Mn_{0.05}Al_{0.03}O$	Dip coating	92	$1.32 \times 10^{+4}$	[34]
$Zn_{0.93}Al_{0.04}Ga_{0.02}Mg_{0.01}O$	RF magnetron sputterin	82	2.8×10^{-3}	[40]
$Zn_{0.90}Mg_{0.03}Mn_{0.01}F_{0.06}O$	Spray pyrolysis	89.53	1.33×10^{-3}	Present work

interests or personal relationships that could have appeared to influence the work reported in this paper.

Data availability

No data was used for the research described in the article.

References

[1] N. Guermat, W. Daranfed, I. Bouchama, N. Bouarissa, Investigation of structural, morphological, optical and electrical properties of Co/Ni co-doped ZnO thin films, J. Mol. Struct. 1225 (2021), 129134, https://doi.org/10.1016/j.molstruc.2020.129134.

[2] R. Sagheer, M. Khalil, V. Abbas, Z.N. Kayani, U. Tariq, F. Ashraf, Effect of Mg doping on structural, morphological, optical and thermal properties of ZnO nanoparticles, Optik 200 (2020), 163428, https://doi.org/10.1016/j.ijleo.2019.163428.

[3] W. Darenfad, N. Guermat, K. Mirouh, A comparative study on the optoelectronic performance of undoped, Mg-doped and F/Mg co-doped ZnO nanocrystalline thin films for solar cell applications, J. Nano Electron. Phys. 13 (2021) 06016, https://doi.org/10.21272/jnep.13(6).06016.

[4] Y. Wang, R. Hao, J. Guo, X. Li, S. Fang, H. Liu, S. Sun, Effect of Mg doping on Cu2ZnSnS4 solar cells prepared by DMF-based solution method, Opt. Mater. 117 (2021), 111211, https://doi.org/10.1016/j.optmat.2021.111211.

[5] X. Si, Y. Liu, W. Lei, J. Xu, W. Du, J. Lin, T. Zhou, L. Zheng, First-principles investigation on the optoelectronic performance of Mg doped and Mg–Al co-doped ZnO, Mater. Des. 93 (2016) 128–132, https://doi.org/10.1016/j.matdes.2015.12.033.

[6] S. Fabbiyola, L.John Kennedy, A.A. Dakhel, M. Bououdina, J. Judith Vijaya, T. Ratnaji, Structural, microstructural, optical and magnetic properties of Mn doped ZnO nanostructures, J. Mol. Struct. 1109 (2016) 89–96, https://doi.org/10.1016/j.molstruc.2015.12.071.

[7] A. Dhivya, R. Yadav, S. Packiam, An Eco-approach synthesis of undoped and Mn doped ZnOnano-photocatalyst for prompt decoloration of methylene blue dye, Mater. Today Proc. 48 (2022) 494–501, https://doi.org/10.1016/j.matpr.2021.02.751.

[8] C. Abed, C. Bouzidi, H. Elhouichet, B. Gelloz, M. Ferid, Mg doping induced high structural quality of sol–gel ZnO nanocrystals: application in photocatalysis, Appl. Surf. Sci. 349 (2015) 855–863, https://doi.org/10.1016/j.apsusc.2015.05.078.

[9] J.S. Seo, J.H. Jeon, Y.H. Hwang, H. Park, M. Ryu, S.H.K. Park, B.-.S. Bae, Solution-Processed flexible fluorine-doped indium zinc oxide thin-film transistors fabricated on plastic film at low temperature, Sci. Rep. 3 (2013) 2085, https://doi.org/10.1038/srep02085.

[10] Z. Pan, P. Zhang, X. Tian, G. Cheng, Y. Xie, H. Zhang, X. Zeng, C. Xiao, G. Hu, Z. Wei, Properties of fluorine and tin co-doped ZnO thin films deposited by sol–gel method, J. Alloy. Compd. 576 (2013) 31–37, https://doi.org/10.1016/j.jallcom.2013.04.132.

[11] Z. Starowicz, A. Zięba, J. Ostapko, M. Wlazło, G. Kołodziej, M.J. Szczerba, G. Putynkowski, R.P. Socha, Synthesis and characterization of Al-doped ZnO and Al/F co-doped ZnO thin films prepared by atomic layer deposition, Mater. Sci. Eng. B 292 (2023), 116405, https://doi.org/10.1016/j.mseb.2023.116405.

[12] A. Mallick, S. Sarkar, T. Ghosh, D. Basak, An insight into doping mechanism in Sn-F co-doped transparent conducting ZnO films by correlating structural, electrical and optical properties, J. Alloy. Compd. 646 (2015) 56–62, https://doi.org/10.1016/j.jallcom.2015.05.070.

[13] M.R. Al Hassan, M.A.Islam Asrafuzzaman, K. Salam, K.F. Amin, M.K. Hasan, Synthesis of spray deposited transition metals doped (Cr, Mn, Fe, Ni, and Cu) compositionally complex ZnO thin films with enhanced band gap and magnetism, Results Mater. 13 (2022), 100263, https://doi.org/10.1016/j.rinma.2022.100263.

[14] Y. Li, Y. Li, Y. Fei, A. Xie, Y. Li, D. Sun, Investigation of properties of ZnO and MgxZn1-xO films prepared by sol-gel method, J. Mol. Struct. 1261 (2022), 132959, https://doi.org/10.1016/j.molstruc.2022.132959.

[15] E. Indrajith Naik, T.S. Sunil Kumar Naik, E. Pradeepa, S. Singh, H.S. Bhojya Naik, Design and fabrication of an innovative electrochemical sensor based on Mg-doped ZnO nanoparticles for the detection of toxic catechol, Mater. Chem. Phys. 281 (2022), 125860, https://doi.org/10.1016/j.matchemphys.2022.125860.

[16] S. Jaballah, M. Benamara, H. Dahman, A. Ly, D. Lahem, M. Debliquy, L. El Mir, Effect of Mg-doping ZnO nanoparticles on detection of low ethanol concentrations, Mater. Chem. Phys. 255 (2020), 123643, https://doi.org/10.1016/j.matchemphys.2020.123643.

[17] H. Wang, A. Wang, Y. Sun, L. Wu, W. li, W. Wang, J. Zhang, L. Feng, Synthesis and characterization of F-doped Mg ZnO films prepared by RF magnetron co-sputtering, Appl. Surf. Sci. 503 (2020), 144273, https://doi.org/10.1016/j.apsusc.2019.144273.

[18] W. Zhang, P. Li, Y. Li, H. Chen, X. Wang, J. Ma, X. Zhao, Structural, optical and electrical properties of sol-gel spin-coated Ga and F Co-doped ZnO films, Thin Solid Films 746 (2022), 139121, https://doi.org/10.1016/j.tsf.2022.139121.

[19] Y. Liu, Q. Zeng, Ch. Nie, H. Yu, Mg and F, Ga co-doped ZnO transparent conductive thin films by dual-target magnetron sputtering: fabrication, structure, and characteristics, J. Alloy. Compd. 907 (2022), 164480, https://doi.org/10.1016/j.jallcom.2022.164480.

[20] N.E. Sung, S.W. Kang, H.J. Shin, H.K. Lee, I.J. Lee, Cu doping effects on the electronic and optical properties of Cu-doped ZnO thin films fabricated by radio

frequency sputtering, Thin Solid Films 547 (2013) 285–288, https://doi.org/10.1016/j.tsf.2012.11.046.
[21] M. Khalfallah, N. Guermat, W. Daranfed, N. Bouarissa, H. Bakhti, Hydrophilic nickel doped porous SnO2 thin films prepared by spray pyrolysis, Phys. Scr. 95 (2020), 095805, https://doi.org/10.1088/1402-4896/aba8c5.
[22] N. Guermat, W. Darenfad, K. Mirouh, N. Bouarissa, M. Khalfallah, A. Herbadji, Effects of zinc doping on structural, morphological, optical and electrical properties of SnO2 thin films, Eur. Phys. J. Appl. Phys. 97 (2022) 14, https://doi.org/10.1051/epjap/2022210218.
[23] N. Guermat, W. Darenfad, K. Mirouh, M. Kalfallah, M. Ghoumazi, Super-hydrophobic F-doped SnO2 (FTO) nanoflowers deposited by spray pyrolysis process for solar cell applications, J. Nano Electr. Phys. 15 (05) (2022) 05013, https://doi.org/10.21272/jnep.14(5).05013.
[24] J. Iqbal, T. Jan, M. Ismail, N. Ahmad, A. Arif, M. Khan, M. Adil, S. Ul-Haq, A. Arshad, Influence of Mg doping level on morphology, optical, electrical properties and antibacterial activity of ZnO nanostructures, Ceram. Int. 40 (2014) 7487–7493, https://doi.org/10.1016/j.ceramint.2013.12.099.
[25] M.H. Majeed, M. Aycibin, A.G. Imer, Study of the electronic, structure and electrical properties of Mg and Y single doped and Mg/Y co-doped ZnO: experimental and theoretical studies, Optik 258 (2022), 168949, https://doi.org/10.1016/j.ijleo.2022.168949.
[26] P. Kumar, H.K. Malik, A. Ghosh, R. Thangavel, K. Asokan, Bandgap tuning in highly c-axis oriented Zn1−xMgxO thin films, Appl. Phys. Lett. 102 (2013), 221903, https://doi.org/10.1063/1.4809575.
[27] W.C. Wu, Y.D. Juang, The optical properties of Mg-doped ZnO quantum dots, Solid State Commun. 350 (2022), 114791, https://doi.org/10.1016/j.ssc.2022.114791.
[28] X. Peng, J. Xu, H. Zang, B. Wang, Z. Wang, Structural and PL properties of Cu doped ZnO films, J. Lumin. 128 (2008) 297–300, https://doi.org/10.1016/j.jlumin.2007.07.016.
[29] R. Subbiah, S. Muthukumaran, V. Raja, Fine-tuning of energy gap, FTIR, photoluminescence and photocatalytic behavior of centella asiatica extract mediated Mn/Mg doped ZnO nanostructure, J. Mater. Sci. Mater. Electron. 30 (2019) 17066–17077, https://doi.org/10.1007/s10854-019-02053-x.
[30] N. Guermat, W. Daranfed, K. Mirouh, Extended wide band gap amorphous ZnO thin films deposited by spray pyrolysis, Ann. Chim. Sci. Matér. 44 (2020) 347–352, https://doi.org/10.18280/acsm.440507.
[31] W. Daranfed, N. Guermat, I. Bouchama, K. Mirouh, S. Dilmi, M.A. Saeed, Effect of the deposition times on the properties of ZnO thin films deposited by ultrasonic spray pyrolysis for optoelectronic applications, J. Nano Electr. Phys. 11 (2019) 6001, https://doi.org/10.21272/jnep.11(6).06001.
[32] K. Huang, Z. Tang, L. Zhang, J. Yu, J. Lv, X. Liu, F. Liu, Preparation and characterization of Mg-doped ZnO thin films by sol–gel method, Appl. Surf. Sci. 258 (2012) 3710–3713, https://doi.org/10.1016/j.apsusc.2011.12.011.
[33] A. Kaushal, D. Kaur, Effect of Mg content on structural, electrical and optical properties of Zn1-xMgxO nanocomposite thin films, Sol. Energy Mater. Sol. Cells 93 (2009) 193–198, https://doi.org/10.1016/j.solmat.2008.09.039.
[34] Y. Babur, A. Tumbul, M. Yıldırım, Chemically derived Zn0.90-xMn0.05Fe0.05AlxO thin films: tuning of crystallite/grain size, optical and dielectric constants and ferromagnetic properties through Al substitutions, Mater. Sci. Semicond. Proc. 84 (2018) 1–9, https://doi.org/10.1016/j.mssp.2018.04.029.
[35] H.B. Ruan, L. Fang, D.C. Li, M. Saleem, G.P. Qin, C.Y. Kong, Effect of dopant concentration on the structural, electrical and optical properties of Mn-doped ZnO films, Thin Solid Films 519 (2011) 5078–5081, https://doi.org/10.1016/j.tsf.2011.01.132.
[36] C.L. Lin, F.H. Wang, H.S. Jhuang, C.F. Yang, Effects of different annealing temperatures on the physical, optical, and electrical characteristics and chemical bonds of Ga and F Co-doped ZnO films, J. Mater. Res. Technol. 9 (3) (2020) 6331–6342, https://doi.org/10.1016/j.jmrt.2020.03.046.
[37] Z. Lu, X. Lv, Q. Xie, Magnetron-sputtered gallium–magnesium–zinc oxide transparent semiconductor thin films: structural, optical and electrical investigation, Optik 265 (2022), 169301, https://doi.org/10.1016/j.ijleo.2022.169301.
[38] A. Hadri, M. Taibi, M. Loghmarti, C. Nassiri, T. Slimani Tlemçani, A. Mzerd, Development of transparent conductive indium and fluorine co-doped ZnO thin films: effect of F concentration and post-annealing temperature, Thin Solid Films 601 (2016) 7–12, https://doi.org/10.1016/j.tsf.2015.11.036.
[39] S.W. Shin, I.Y. Kim, G.V. Kishor, Y.Y. Yoo, Y.B. Kim, J.Y. Heo, G.S. Heo, P.S. Patil, J.H. Kim, J.Y. Lee, Development of flexible Mg and Ga co-doped ZnO thin films with wide band gap energy and transparent conductive characteristics, J. Alloy. Compd. 585 (2014) 608–613, https://doi.org/10.1016/j.jallcom.2013.09.133.
[40] Y. Liu, S. Zhu, Preparation and characterization of Mg, Al and Ga co-doped ZnO transparent conductive films deposited by magnetron sputtering, Results Phys 14 (2019), 102514, https://doi.org/10.1016/j.rinp.2019.102514.